For. Stud. China, 2006, 8(1): 35–40
DOI 10.1007/s11632-006-0007-6

Preparation and characterization of wood/montmorillonite nanocomposites

Lü Wen-hua[1,2,3] *Zhao Guang-jie*[1*] *Xue Zheng-hua*[1]

[1]College of Material Science and Technology, Beijing Forestry University, Beijing 100083, P. R. China
[2]Research Institute of Wood Industry, Chinese Academy of Forestry, Beijing 100091, P. R. China
[3]Faculty of Wood Science and Decoration Engineering, Southwest Forestry College, Kunming 650224, P. R. China

Abstract With montmorillonite (MMT) organically modified as organophilic MMT (OMMT) and water-soluble phenol formaldehyde resin (PF) as intermediate, Chinese fir (*Cunninghamia lanceolata*) wood/MMT nanocomposites (WMNC) were prepared via nano intercalation compounding and characterized by XRD, SEM and FTIR. Results show that: 1) the preparation of OMMT is very successful; 2) the self-made PF can effectively intercalate into MMT to increase markably its gallery distance and even exfoliate its nano silicate laminae; 3) the XRD analysis indicates that some exfoliated MMT enters the non-crystallized region of microfibrils in wood cell walls and the crystallinity degree of wood in WMNC decreases; 4) the SEM graphs show that multiform MMT exists in WMNC. Some grains block in wood cell lumen, some layers adhere to the wood surface of the inner cell wall and some exfoliated nanolaminae even insert into wood cell walls; and 5) the FTIR analysis suggests that MMT and wood in WMNC perhaps interact via certain chemical bonding.

Key words Chinese fir (*Cunninghamia lanceolata*), montmorillonite (MMT), nano intercalation compounding, preparation and characterization

1 Introduction

Nano science and technology open a completely new way to develop wood composites (Zhao and Lü, 2003). It is a challenging, attractive and critical field to develop high-value-added and multifunctional wood nanocomposites. The intercalation nanocompounding of montmorillonite (MMT) and polymers has been widely studied and its theory and technology are relatively mature (Alexandre et al., 2000; Li et al., 2002). Compounding wood with MMT on a nano-scale will greatly improve wood and even provide wood with new functions and utilization. Wood chiefly consists of cellulose, hemicellulose and lignin. Due to cellulose having a high degree of crystallinity, wood is of low plasticity (Hilliz and Rozsa, 1978), its processing is markedly different from that of synthetic polymers (Yu, 1996). Wood is a natural porous composite with macrospaces as cell lumen and vessels and microspaces as cell interspaces (Zhao and Lü, 2003). Adding various heterogeneous materials into wood to make composites has been an important method to improve its quality (Saka and Ueno, 1997; Chen et al., 2003). One of the most important methods to modify wood is to impregnate wood with water-soluble reagents (Wang, 2003). According to their chemical composition and structure (Wen, 1989; Li, 2003), the interaction between wood and MMT is somewhat weak. MMT could be modified to be organophilic and then be further intercalated or delaminated by polymers (Wu et al., 1999; Alexandre et al., 2002). With the help of certain polymers, MMT nano silicate layers can be delaminated and introduced into wood. The key technology is how to exfoliate MMT nanolaminae and how to introduce the exfoliated nanolaminae into wood (Lü and Zhao, 2004). In this study, a water-soluble phenol formaldehyde resin (PF) of low molecular weight was synthesized and selected as the medium to prepare wood/MMT nanocomposites (WMNC). With MMT organically modified and water-soluble PF as intermediate, WMNC were prepared via intercalation compounding and characterized by XRD, SEM and FTIR.

2 Materials and methods

2.1 Materials

The clay used in this study was industrially purified and modified Na-MMT. Its cation exchange capacity was 90 meq/100 g and its nominal tactoid aggregate size 300-mesh. The organic intercalation agent C_{18} was synthesized with hydrochloric acid and octadecylamine. The low-molecular-weight PF was synthesized with phenol, formaldehyde and sodium hydrox-

*Author for correspondence. E-mail: zhaogjws@263.net

ide. Chinese fir (*Cunninghamia lanceolata*) wood came from Fujian Province. Its air-dry density was 0.365 g·cm^{-3} and its air-dry moisture content 9%. Wood sample dimensions were 20 mm×20 mm×20 mm.

2.2 Preparation of organo-MMT (OMMT)

Organically modified MMT was prepared by cation exchange of Na-MMT with organic ammonium salts C_{18} in distilled water. A desired amount of powdery Na-MMT was dispersed into distilled water at 60°C with mechanical stirring for a couple of hours. C_{18} was prepared by mixing octadecylamine with a hydrochloric acid solution. The mixture was stirred at 80°C until a clear solution was obtained. An amount of 1.5 CEC C_{18} solution was added dropwise to the Na-MMT suspension solution with vigorous stirring at a rate of approximately 10 mL·min^{-1}. The stirring was continued at 80°C for 1.5 h and the resulting white precipitate was collected in a Buchner funnel by suction filtration. The precipitate was repeatedly rinsed with hot distilled water to remove any excessive intercalation agent, until no white precipitate was formed in the filtrate when tested with a drop of 0.1 mol·L^{-1} silver nitrate ($AgNO_3$) solution. Then the resulting product was vacuum-dried to a constant weight. Finally, it was ground into fine particles and the fraction through a 300-mesh sieve was collected by mechanical sifting and the final OMMT obtained.

2.3 Synthesis of water-soluble PF

The prescribed melted phenol and sodium hydroxide was added into a reaction pot with mechanical stirring. When the temperature decreased below 50°C, 80% of the total amount of formaldehyde was poured into the pot. In succession, the pot was heated at an even rate and held at 50°C for 20 min, at 60°C for 50 min and at 70°C for 20 min. Then the remaining 20% formaldehyde was poured into the reaction pot and the pot was steadily heated up to 90°C and left in this condition. One hour later, a sample of about 1 mL was taken from the pot to measure its water solubility. With the reaction going on, the interval to take samples was reduced. When the water solubility multiple of samples reached 3.5, the reaction was immediately stopped. PF was prepared and its main quality parameters were measured. The PF was kept at a low temperature.

2.4 Preparation of WMNC

The low-molecular-weight PF resin, as described above, was blended with distilled water to prepare the PF solution with a certain concentration. To this solution a desired amount (<3% wt) of OMMT was added and the impregnating solution for wood was prepared. First, wood samples were prevacuumed under negative pressure of 0.095 MPa for 30 min. Second, the impregnating solution was introduced into a vacuum container. After the samples had been sufficiently soaked, they were vacuumed again and the negative pressure was kept for 30 min. Then the samples were taken out from the impregnating solution and a second vacuum was performed for several minutes to clear the wood surface. After being air-dried for a while, the samples were cured at 120°C for 3 h and WMNCs obtained.

2.5 Measurements

All samples were first ground into fine powder with an agate mortar and then sifted through a 100-mesh sieve for XRD, SEM and FTIR analysis. The analyses were performed under the following conditions: 1) the XRD analysis: XRD-6000 produced by SHIMADZU Corp., Japan, continuing scanning, CuKα radiation (λ = 0.154 nm), radiation tube voltage of 40 kV, radiation tube current of 30 mA, 2θ scanning range of 1.5°–40°, scan rate of 4° per minute and scan step of 0.1°; 2) the SEM analysis: Quanta 200HV SEM produced by FEI Corp., USA, ion-spraying gilding in vacuum; (3) the FTIR analysis: Tensor27 FTIR produced by Bruker Corp., Germany, KBr, scanning frequency of 32, resolution of 4 cm^{-1}, scanning range of 400–4,000 cm^{-1}.

3 Results and discussion

3.1 The XRD analysis I (cps)

The XRD pattern of OMMT is shown in Fig. 1. The diffraction peak of Na-MMT (curve a) is at 2θ of 6.15°. According to the Bragg equation $2d\sin\theta = n\lambda$ (Alexandre and Dubois, 2000), the gallery distance of Na-MMT is calculated to be 1.435 nm. As for OMMT (b), the first grade diffraction peak is at 2θ of 3.07° corresponding to an increased gallery distance of 2.875 nm. It is concluded that the sodium cations between MMT layers are substituted by the organic alkyl cations of an intercalation agent (Kornmann et al., 2001). The characteristic diffraction peak of OMMT is sharp and single, which suggests that the cation exchange is very efficient. The plateau near 2θ of 5° indicates that a non-uniform intercalation of organic cations exists in MMT.

The powdery OMMT and PF solutions were first fully blended at a desired weight ratio and kept for a certain time to ensure the full penetration of PF. Then it was spread on glass sheets to make samples. After the samples were vacuum cured at 140°C for 2 h, PF/MMT composites were prepared. The XRD pat-

terns of PF/MMT composites are expressed in Fig. 2, in which curves a and b are of the same PF/MMT compounding system. It is seen from curve a that the first grade diffraction peak of OMMT deviates from 3.07° to 2.93° of 2θ, correspondingly the calculated gallery distance of MMT increases from 2.875 to 3.346 nm. Seen from curve b, there is no obvious diffraction peak in the range from 2° to 10° of 2θ. There will be two conditions (Vaia and Giannelis, 1997; Fu and Qutubuddin, 2001), that is, the MMT gallery is fully expanded to a large space that cannot be detected by XRD, or the MMT laminae are delaminated to be free and no crystal diffraction peak appears. Accordingly the PF/MMT compound is probably partially intercalated and partially exfoliated. Based on the chemical structure, both MMT and PF have hydroxyls (Choi et al., 2000; Lin and Ma, 2000; Wu et al., 2001) and their compatibility is good. The hydroxyls in PF perhaps combine with the oxygen atoms on the MMT surface via hydrogen bonding.

The XRD patterns for PF-impreg, simple physical PF-impreg-OMMT blend and WMNC are respectively depicted as curves a, b and c in Fig. 3. The skeleton substance of wood cell walls is cellulose. Cellulose has a multiphase crystalline structure with crystalline and amorphous regions. Cellulose is of a unitary oblique crystal system with a distinct XRD pattern (Li, 2003). Since the boundary between the crystalline and amorphous regions is not apparent, the correlated transformation in the XRD pattern is gradual. As shown in Fig. 3, PF-impreg (a) has two wide diffraction peaks near 15.41° and 21.93°of 2θ and a small diffraction peak near 37.75° of 2θ. The peak near 21.93° of 2θ reflects the maximum diffraction of the 002 crystal plane of cellulose; the trough near 18° of 2θ is attributed to the amorphous region. The small peak near 37.75°of 2θ is due to the diffraction of the 040 crystal plane of cellulose. Because the glucose molecule plane in cellulose is parallel to the 002 crystal plane, the diffraction of the 002 crystal plane is stronger than that of the 040 crystal plane (Li, 2003). Curve b is that of a simple physical PF-impreg-OMMT blend, in which the characteristic diffraction peak of OMMT at 3.38° of 2θ occurs with no change. As for WMNC (curve c), the corresponding peak disappears, which denotes that the MMT gallery space is greatly expanded, or MMT nanolaminae are exfoliated free (Chin et al., 2001). Compared with curves a and b (Fig. 3), curve c has the following changes: diffraction near 2θ = 16°–18° intensifies to a plateau from trough of PF-impreg (a); a small and sharp peak occurs near 2θ = 17°; the diffraction peaks of the cellulose 002 crystal plane near 15.41° and 21.93° of 2θ become dull; and the small peak of the cellulose 040 crystal plane near 37.75° of 2θ almost disappears. All this suggests that the crystallinity degree of wood in WMNC decreases, MMT exfoliates and some silicate nanolaminae are inserted into the amorphous region of cellulose of wood cell walls.

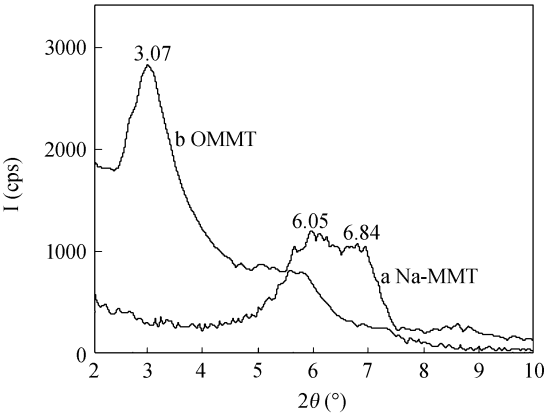

Fig. 1 XRD analysis of MMT before and after the organic modification

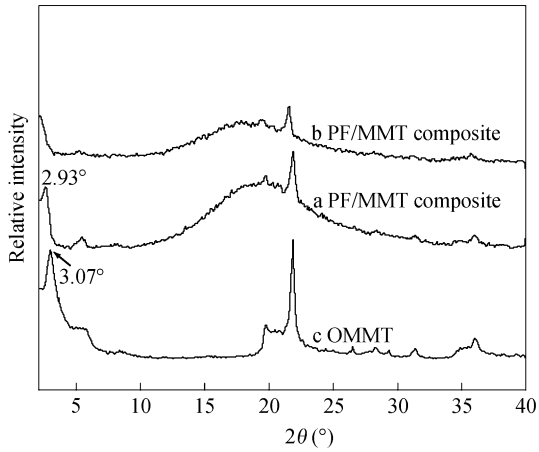

Fig. 2 XRD analysis of OMMT and PF/MMT composites

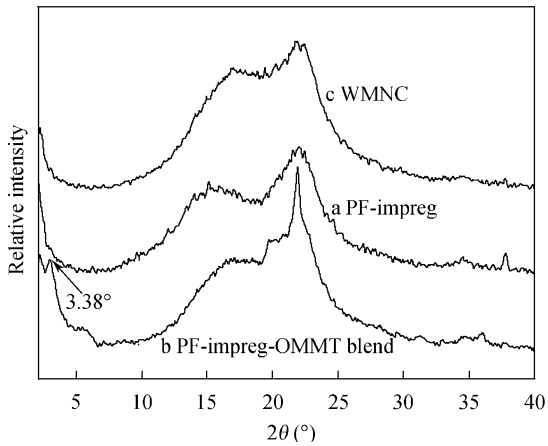

Fig. 3 XRD analysis of PF-impreg, PF-impreg-OMMT blend and WMNC

3.2 The SEM analysis

SEM was applied further to discern the state of MMT. Fig. 4 shows the 24,000-time magnified SEM graphs

of inorganic Na-MMT (A) and C_{18}-organically modified OMMT (B). As shown, the change of appearance in MMT is very distinct before and after the organic modification. The inorganic Na-MMT (A) is regularly layer-aggregated with obvious crystal characteristics and its nanolayer surfaces are plainly extended. But the nanolayers in OMMT (B) are irregularly and loosely aggregated with curled edges, a non-flat surface and are even exfoliated free. SEM graphs prove that the organic intercalation agent enters the MMT gallery. The MMT interlayer space is markedly enlarged and the partial MMT nanolayers are exfoliated and freely dispersed. Apparently the organic modification of Na-MMT is very successful.

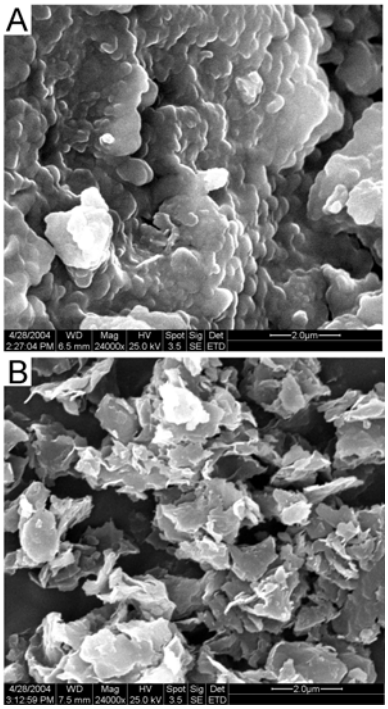

Fig. 4 SEM analysis of Na-MMT before and after the organic modification. A: inorganic Na-MMT (24,000×); B: C_{18}-OMMT (24,000×).

The SEM graphs of Fig. 5 result from one PF/MMT composite. Figure 5A characterizes an intercalated form, in which MMT galleries are apparently enlarged but MMT still retains its aggregated crystalline structure. Figure 5B characterizes an exfoliated form, in which delaminated nano clay layers are randomly dispersed and fully compounded with PF. The PF/MMT nanocomposites in this study are partially intercalated and partially exfoliated. Just as the XRD and SEM analyses denote, the organic modification of Na-MMT is non-uniform, the free nanolamellae and the crystalline aggregates, with very different interlayer distances, coexist. Accordingly, the intercalation compounding of PF and OMMT is also non-uniform and the intercalated and exfoliated forms occur simultaneously in a composite. As for different compounding systems, the ratio of the two forms is different. Its compounding phases have the largest and sufficient contact, but the exfoliated nanocomposite is most desired.

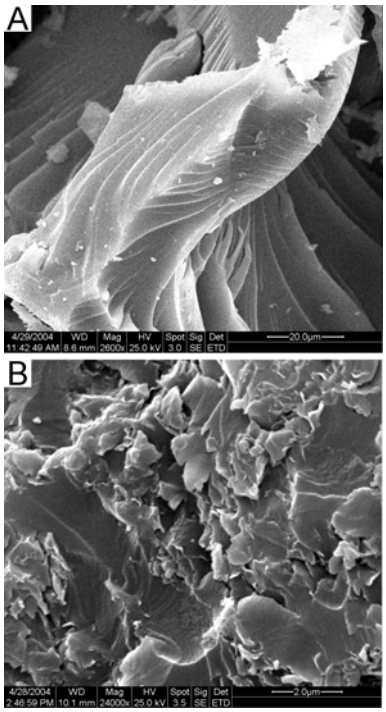

Fig. 5 SEM analysis of PF/MMT compounding system. A: intercalated PF/MMT (2,600×); B: exfoliated PF/MMT (24,000×).

The SEM graphs of WMNC (white arrows pointing to MMT lamellae) are shown in Fig. 6. Figure 6A is the wood cross section in WMNC. It is seen that, the clay layers are either filling the wood cell lumen, are adsorbed into the inner surface of wood cell walls, or inserted into wood cell walls. Figure 6B is a filled wood pit in WMNC. As shown, the MMT nanolamellae are either closely attached to the inner surface of cell walls filling the pit canal, or are inserted into wood cell walls. Due to the non-uniformity of the OMMT modification, the PF intercalation and wood impregnation, the morphology and distribution of MMT in WMNC are very diverse; big MMT grains and free nano clay lamellae are in concurrence.

3.3 The FTIR analysis

The FTIR spectrum of organophilic-MMT is shown in Fig. 7. As depicted, the organic modification caused several new absorption peaks. The strong absorption near 2,920 and 2,851 cm^{-1} is attributed to the stretching and contracting vibration of $-CH_2-$ groups and the absorption near 1,472 cm^{-1} reflects the bending vibra-

tion of $-CH_2-$ groups (Shen, 1982). This indicates that the organic groups of intercalation agents do intercalate into MMT galleries and the amount of substitution is large. The stronger the absorption peaks related to $-CH_2-$ groups, the better the modifying effect (Wu, 2002). Evidently, the organic modification is very successful in this study. The vibration absorptions of Si−O−Si and Si−O−Al groups in MMT crystal lattice near 1,031, 907, 796, 522 and 468 cm^{-1} (Wen, 1989) have almost no obvious change before and after the organic modification. The absorption near 3,626 cm^{-1} relating to MMT structural water, remains almost unchanged, while the absorption near 3,400 and 1,630 cm^{-1} pertaining to adsorbing water in MMT galleries decreases markedly. It is concluded that the hydrophobic intercalation agent enters MMT galleries and expels most adsorbing water present, but it has little effect on the structural water of MMT crystal lattices.

Figure 8 shows the FTIR difference spectrum by subtracting the PF spectrum from the PF/MMT composite spectrum. It reflects the characteristic adsorption peaks of clay crystal lattices, such as the Si−O−Si vibrating adsorption near 618, 1,033 and 1,085 cm^{-1} and the Si−O−Al vibrating adsorption near 463 cm^{-1}. Compared with PF-impreg, the PF/MMT composite has weaker ether-linking vibrating adsorption near 1,210 cm^{-1} and stronger −OH vibrating adsorptions near 3,727, 3,450 and 1,657 cm^{-1} (Wu, 2002; Huang and Jiao, 2003). It is considered that some strong linking occurs between MMT and PF molecules via their oxygen atoms.

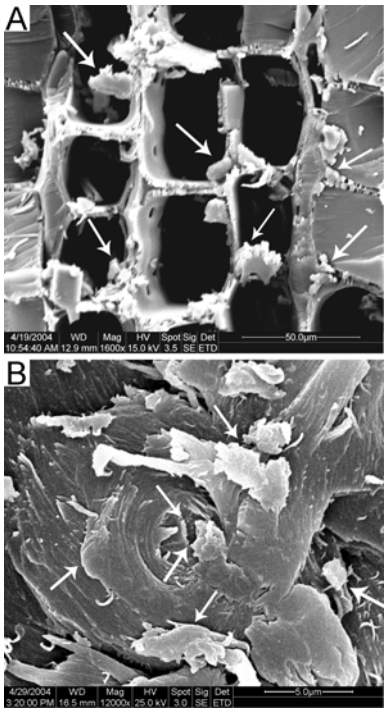

Fig. 6 SEM analysis of WMNC (arrows pointing to clay layers). A: wood cross section (1,600×); B: a wood pit (12,000×).

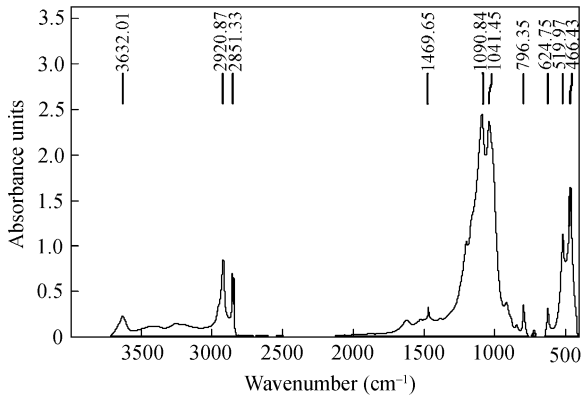

Fig. 7 FTIR analysis of the organically modified C_{18}-OMMT

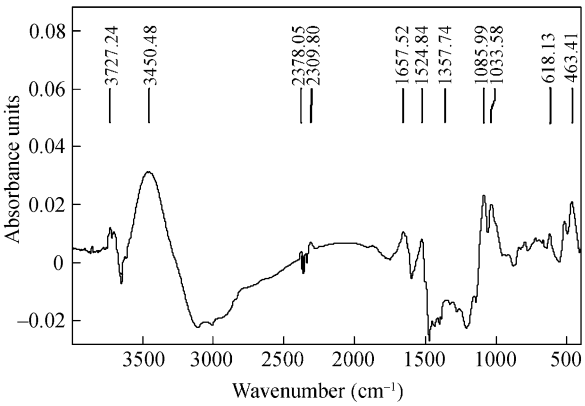

Fig. 8 FTIR difference spectrum between PF and PF/MMT compound

The FTIR difference spectrum is generated by subtracting the PF-impreg spectrum from the WMNC spectrum (Fig. 9). The Si−O−Si and Si−O−Al vibrating adsorptions near 1,042, 757 and 464 cm^{-1} indicate that there is inorganic MMT in WMNC. The −OH vibrating adsorption near 3,304 cm^{-1}, the −C=O vibrating adsorptions near 1,738, 1,153 and 1,042 cm^{-1} and the −C−O vibrating adsorption near 1,240 cm^{-1} all increase in WMNC. It can be concluded that some chemical combinations, related to oxygen atoms, come into being between MMT and wood in WMNC.

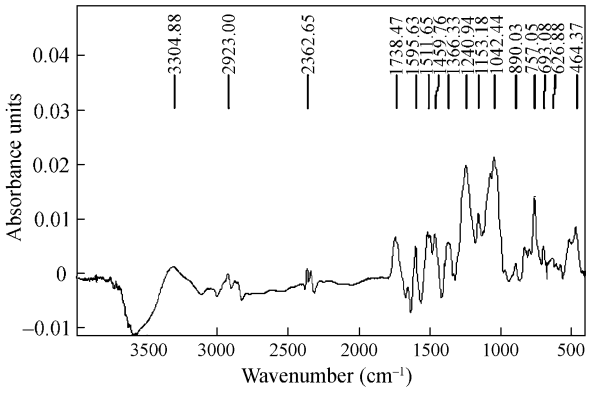

Fig. 9 FTIR difference spectrum between PF-impreg and WMNC

4 Conclusions

Based on the results from this study, several conclusions were draw as follows:

1) The preparation of OMMT is very successful.
2) The PF synthesized in our laboratory can effectively intercalate into OMMT to make its gallery distances increase markedly and even make its silicate layers exfoliated.
3) XRD analyses indicate that the crystallinity degree of wood in WMNC decreases. This accounts for the fact that MMT exfoliates and some nano silicate layers enter into the non-crystallized region of microfibrils in wood cell walls.
4) SEM graphs for WMNC show that some MMT grains block in wood cell lumen, some MMT layers adhere to the inner surface of wood cell walls and some exfoliated MMT layers even insert into wood cell walls.
5) FTIR analyses suggest that MMT and wood interact via certain chemical linkages in WMNC.

Acknowledgement

This study was financially supported by the National Natural Science Fundation of China (Grant No. 30070606).

References

Alexandre M, Dubois P. 2000. Polymer-layered silicate nanocomposites: preparation, properties and uses of a new class of materials. Mat. Sci. Eng. R., 28(1/2): 1–63

Alexandre M, Dubois P, Sun T, Garces J M, Jérôme R. 2002. Polyethylene-layered silicate nanocomposites prepared by the polymerization-filling technique: synthesis and mechanical properties. Polymer, 43(8): 2,123–2,132

Chen Z L, Wang Q, Zhang X L, Zuo T Y, Fu F, Ye K L. 2003. Recent development of research on wood/inorganic nonmetallic composites. J. Beijing Univ. Technol., 29(1): 116–121 (in Chinese with an English abstract)

Chin I J, Thurn-Albrecht T, Kim H C, Russell T P, Wang J. 2001. On exfoliation of montmorillonite in epoxy. Polymer, 42(13): 5,947–5,952

Choi M H, Chung I J, Lee J D. 2000. Morphology and curing behaviors of phenolic resin-layered silicate nanocomposites prepared by melt intercalation. Chem. Mater., 12(10): 2,977–2,983

Fu X, Qutubuddin S. 2001. Polymer-clay nanocomposites: exfoliation of organophilic montmorillonite nanolayers in polystyrene. Polymer, 42(2): 807–813

Hilliz W E, Rozsa A N. 1978. The softening temperature of wood. Holzforschung, 32(2): 68–73

Huang F R, Jiao Y S. 2003. Phenol Formaldehyde Resin and Its Application. Beijing: Chemical Industry Press (in Chinese)

Kornmann X, Lindberg H, Berglund L A. 2001. Synthesis of epoxy-clay nanocomposites: influence of the nature of the clay on structure. Polymer, 42(4): 1,303–1,310

Li J. 2003, Wood Spectroscopy. Beijing: Science Press (in Chinese)

Lin J, Ma C M. 2000. Thermal degradation of phenolic resin/silica hybrid creamers. Polym. Degrad. Stabil., 69(2): 229–235

Li Q, Lin W W, Song C F. 2002. Preparation, characteristics and application of polymer matrix nanocomposites. Mater. Sci. Eng., 20(1): 108–110, 67

Lü W H, Zhao G J. 2004. Design of Wood/Montmorillonite (MMT) Intercalation Nanocomposite. For. Stud. China., 6(1): 54–62

Saka S, Ueno T. 1997. Several SiO_2 wood-inorganic composites and their fire-resisting properties. Wood Sci. Technol., 31(6): 457–466

Shen D Y. 1982. Application of Infrared Spectroscopy in Polymer Study. Beijing: Science Press (in Chinese)

Vaia R A, Giannelis E P. 1997. Polymer melt intercalation in organically-modified layered silicaters: model predictions and experiments. Macromolecules, 30(25): 8,000–8,009

Wang Q W. 2003, Wood Fire-retardant Technology. Harbin: Northeast Forestry University Press (in Chinese)

Wen L. 1989, Mineral Infrared Spectroscopy. Chongqing: Chongqing University Press (in Chinese)

Wu B H, Wang Y Z, Yu D S. 1999. Preparation and Characterization of Organic Modified Montmorillonite. Petrochem. Technol., 28(3): 1–6 (in Chinese with an English abstract)

Wu G. 2002, Material Structure Characterization and Application. Beijing: Chemical industry Press (in Chinese)

Wu Z G, Zhou C X, Cheng B J. 2001. Synthesis of novolac/montmorillonite nanocomposite by *in situ* suspension polymerization. China Synthetic Rubber Ind., 24(4): 233–238 (in Chinese with an English abstract)

Yu Q Y. 1996. Chemical modification converting wood into thermoplastic and thermosetting materials. Prog. Chem., 8(4): 331–339 (in Chinese with an English abstract)

Zhao G J, Lü W H. 2003. Nanoscale in wood, nanowood and wood-inorganic nanocomposites. For. Stud. China., 5(1): 44–48

(Received October 12, 2005 Accepted December 26, 2005)